

Cite this: *CrystEngComm*, 2011, **13**, 5071

www.rsc.org/crystengcomm

PAPER

Construction and isomeric transformation of polyoxometalates directed by 1, ω -bis(pyridinium)alkane templates†

Yun-Yin Niu,^{*a} Ling-Fang Wang,^a Xiao-Rui Lv,^a Hai-Juan Du,^a Yong-Zhen Qiao,^a Hong-Mei Wang,^a Li-Sha Song,^a Ben-Lai Wu,^a Hong-Wei Hou^a and Seik Weng Ng^b

Received 24th February 2011, Accepted 21st April 2011

DOI: 10.1039/c1ce05245d

Ten novel inorganic–organic hybrid polyoxometalates, namely, [1,3-bis(pyridinium) propane]₂[α -Mo₈O₂₆] (**1**), [1,4-bis(pyridinium)butane]₂[1D-Mo₈O₂₆] (**2**), [1,5-bis(pyridinium)pentane]₂[θ -Mo₈O₂₆] (**3**), [1,6-bis(pyridinium)hexane]₂[1D-Mo₈O₂₆] (**4**), [1,7-bis(pyridinium)heptane]₂[β -Mo₈O₂₆] (**5**), [1,8-bis(pyridinium)octane]₂[θ -Mo₈O₂₆] (**6**), [1,9-bis(pyridinium)nonane]₂[(α + β)-Mo₈O₂₆] (**7**), [1,10-bis(pyridinium)decane]₂[β -Mo₈O₂₆] (**8**), [1,11-bis(pyridinium)undecane]₂[β -Mo₈O₂₆] (**9**), [1,12-bis(pyridinium)dodecane]₂[γ -Mo₈O₂₆] (**10**), (Scheme 1) were synthesized by cation templated self-assembly with octamolybdate anions under hydrothermal reaction conditions. Crystal data analysis revealed that these compounds were all composed of discrete organic cations and polyacid anions [Mo₈O₂₆]⁴⁻ interacting by electrostatic and hydrogen bond interactions. Interestingly in these compounds the anion fraction could take on α -, β -, θ -, γ -[Mo₈O₂₆]⁴⁻ 0D isomers or rare 1D- polymeric frameworks with a simple length modification of the alkane components. Moreover, these polyacid compounds had definite catalytic activities on the oxidation reaction of acetaldehyde to acetic acid and the relationship of structure/catalytic activities were initially demonstrated.

Introduction

The rational design and synthesis of organic–inorganic hybrid materials had attracted considerable interest in the last few years not only from a structural point of view, but also due to their potential applications in different areas such as catalysis, medicine, sorption, electrical conductivity, magnetism and photochemistry.^{1–7} One synthetic strategy for design of inorganic–organic hybrid materials was to select suitable inorganic building blocks and organic templates with structure-directing functions. Polyoxometalates (POMs), as one kind of significant metal oxide cluster of nanosize and abundant topologies have been employed as inorganic building blocks for the construction of supramolecular arrays with various organic ligands.^{8–11} These supramolecular assemblies possessed interesting 1–3 dimensional structures, and exhibited potential applications in many fields.^{12–15} Therefore, the functionality of inorganic–organic hybrid materials based on POMs could be multiplied by the

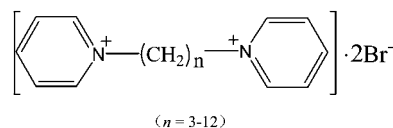
incorporation of organic and inorganic counterparts into one structural unit.¹⁶

Recently, a great deal of research effort has been paid to the functionalization of POMs by incorporating an organic component or transition metal complex,¹⁷ and more organic–inorganic hybrid materials were successfully prepared by using POMs as building blocks. Octamolybdates provided an important branch of polyoxomolybdate chemistry due to their varied structural patterns in the solid state. Up to now, eight isomeric forms including the α -, β -, γ -, δ -, ϵ -, ζ -, η -, and θ - octamolybdates had been prepared in discrete presentations.^{18–26} In this paper, as a first attempt at the systematic use of 1, ω -bis(pyridinium)alkane dications ($\omega = 3–12$) (Scheme 1) as templated microstructural tuners to synthesise polyacid species,²⁷ ten octamolybdates supramolecular isomers were created and presented simultaneously in the same work. Moreover, it was indicated that these polyacid compounds all had definite catalytic activities through the investigation of the oxidation reaction of acetaldehyde to acetic acid.

^aDepartment of Chemistry, Zhengzhou University, Zhengzhou, 450001, P. R. China. E-mail: mailto:niuyy@zzu.edu.cn

^bDepartment of Chemistry, University of Malaya, 50603 Kuala Lumpur, Malaysia

† Electronic supplementary information (ESI) available: Selected bond distances and angles for **1–10**, structural figures of **3**, **4**, **8**, **9**, experimental and simulated powder XRD patterns, and the detailed crystallographic data and structural refinement parameters for **1–10**. CCDC reference numbers 814192–814201. For ESI and crystallographic data in CIF or other electronic format see DOI: 10.1039/c1ce05245d



Scheme 1 Schematic representation of the 1, ω -bis(pyridinium)alkane dications ($n = 3–12$).

Results and discussion

Discussion of synthesis

All this series of compounds were hydrothermally synthesized by a large number of experiments. Preparation of compounds was mainly affected by several factors:

(1) **pH value.** From the perspective of the synthetic experiments, pH played an important role in the formation of the molybdenum oxygen anions. Compounds 1–3 were obtained at an initial pH value of 5; while compounds 4–10 were prepared adjusting with dilute HNO₃ to pH 3–3.5. Otherwise only light yellow powders were obtained at a pH value of 5. This could be related to the existence of different states of molybdenum oxide anions at different pH and cation templated conditions. (2) **Temperature.** It was shown that the best temperature for the preparation of these compounds was in the range of 120–160 °C. Compounds 1 and 2 were obtained at an optimal reaction temperature of 120 °C, while the optimal range of reaction temperature for other several compounds was 150–160 °C. At low heating temperature only some light yellow powders were obtained, but the organic cations decomposed thermally under the high temperature and non-crystal product formation occurred. Thus, the temperature was also a key factor in this hydrothermal reaction. (3) **Organic cations.** The organic cations played a structure directing, template and charge counter-balancing role in the synthetic process of the compounds. Different organic cations required different crystallization temperatures and pH conditions. The shorter the length of the alkyl chain in 1,ω-bis(pyridinium) alkanes was, the lower the reaction temperature required is, and the slightly higher the pH value. (4) **Reaction time.** Reaction time affected the formation of the crystal nucleus, and the crystal size. It was shown that the complete crystal shape of compound 1 appeared in a reaction period of 3-days, while the complete crystals of other compounds were obtained in 4 days. No complete crystals of 2–10 except some powders were obtained in a reaction time of less than 4 days.

In the synthesis process, the octamolybdate product of $n = 1$ and 2 could not be obtained as the organic cation 1,1'-bis(pyridinium)methane broke up into pyridine under hydrothermal conditions, so that the crystalline product obtained at room temperature was the pyridinium cation. Meanwhile, the self assembled reaction of 1,2-bis(pyridinium)ethane cation did not form a crystal of the hybrid product under the above experimental conditions, with only precipitation being observed.

Description of crystal structures

Structure of [1,3-bis(pyridinium)propane]₂[α-Mo₈O₂₆] (1) with α-octamolybdate isomer. Single crystal X-ray diffraction analysis revealed that compound 1 consisted of 1,3-bis(pyridinium)propane cations and the polyanion α-[Mo₈O₂₆]⁴⁻ held together by electrostatic interactions (Fig. 1a). The [Mo₈O₂₆]⁴⁻ anion lies about an inversion centre. In the crystal of compound 1, the alkyl chain of 1,3-bis(pyridinium)propane dication existed in an *anti-gauche* conformation. The polyanion [Mo₈O₂₆]⁴⁻ is composed of two centrosymmetric subunits [Mo₄O₁₃]²⁻. Each subunit consisted of three MoO₆ octahedra and one MoO₄ tetrahedron by edge-sharing and corner-sharing. The oxygen atoms within the [Mo₈O₂₆]⁴⁻ cluster could be divided into three sets according to

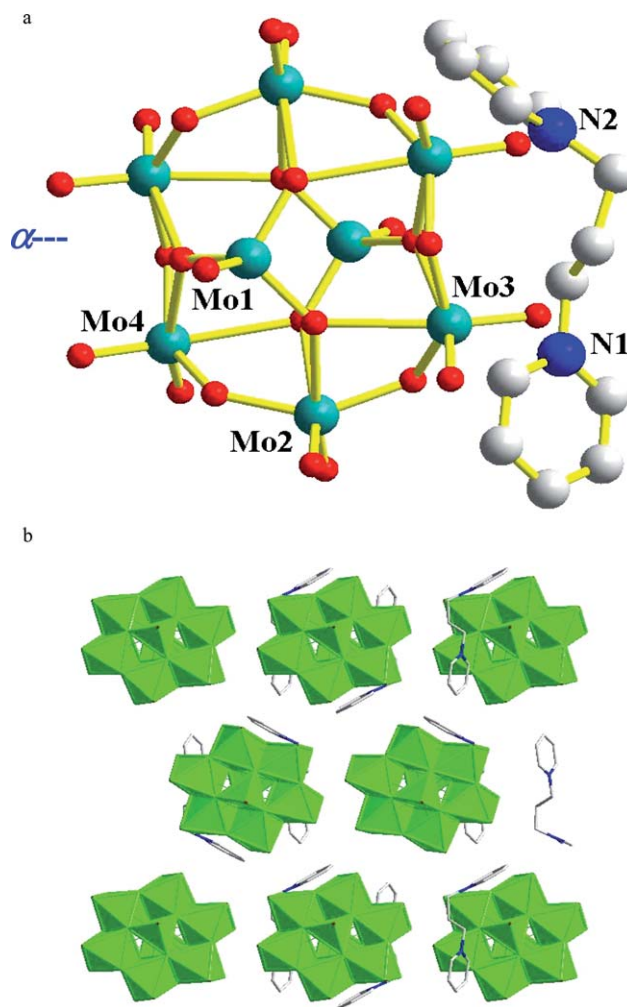


Fig. 1 a Structure of compound 1 with atomic labeling. Symmetry codes: #1 – $x + 1, -y + 1, -z + 1$. All H atoms were omitted for clarity. b Packing of compound 1 viewing along the crystallographic [100] direction. All H atoms were omitted for clarity.

their bonding features, namely, terminal oxygen atoms with Mo–O distances of 1.689–1.704 Å, double bridging oxygen atoms with Mo–O distances of 1.876–1.928 Å, and triple bridging oxygen atoms with Mo–O distances of 1.778–2.525 Å. The Mo–O average distance of the three sets was 1.697, 1.940, and 2.095 Å, respectively. The results indicated that MoO₆ octahedron and MoO₄ tetrahedron showed definite distortion. Along the crystallographic *a* axis, each polyanion [Mo₈O₂₆]⁴⁻ cluster was surrounded by twin organic cations (Fig. 1b). Along the crystallographic *c* axis, polyanions [Mo₈O₂₆]⁴⁻ cluster and organic cations showed a parallel array, and mutually filled in each other's interspaces, giving rise to form a three-dimensional supramolecular network by electrostatic interactions and intermolecular interactions.

Structures of [1,4-bis(pyridinium)butane]₂[1D-Mo₈O₂₆] (2), and [1,6-bis(pyridinium)hexane]₂[1D-Mo₈O₂₆] (4) with 1D anion chain. Single crystal X-ray diffraction analysis revealed that compound 2 was composed of independent 1,4-bis(pyridinium)butane cation and infinite polyanion [Mo₈O₂₆]⁴⁻ (Fig. 2a). In the crystal,

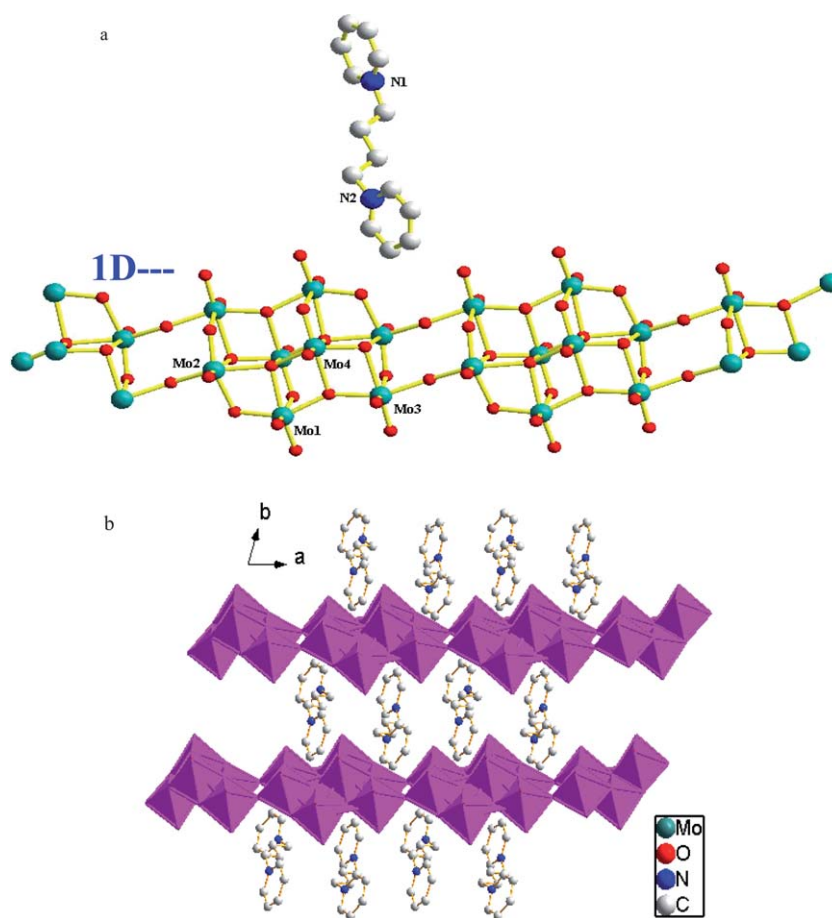


Fig. 2 **a** Structure of compound **2** with atomic labeling. Symmetry codes: #1 $x - 1, y, z$ #2 $-x + 2, -y + 1, -z + 1$. All H atoms were omitted for clarity. **b** The supramolecular structure diagram of compound **2** along the crystallographic c axis with ball and stick and polyhedral style. Polyacid $[\text{Mo}_8\text{O}_{26}]^{4-}$ anion represented chain-shape structure in **2**. All H atoms were omitted for clarity.

the alkyl chain of 1,4-bis(pyridinium)butane dication existed in an *anti-anti-anti* conformation. The $[\text{Mo}_8\text{O}_{26}]^{4-}$ anion consisted of a twin-cage structure arranged as two centrosymmetric subsets of $[\text{Mo}_4\text{O}_{13}]^{2-}$. Each subunit contained four MoO_6 octahedra, but the Mo–O distances were unequal. The results showed that MoO_6 octahedron showed definite distortion from the ideal geometry, which may be related to the introduction of the organic cation and the changed oxygen atoms sets around the Mo atoms. The anion $[\text{Mo}_4\text{O}_{13}]^{2-}$ subunit consisted of four sets of Mo atoms which were coordinated with different oxygen atoms: oxygen atoms sets around Mo1 include two terminal oxygen atoms, two double bridging oxygen atoms, one triple bridging oxygen atom and one quadruple bridging oxygen atom. The Mo(1)–O (3), Mo(1)–O(1), Mo(1)–O(4), Mo(1)–O(12)#1, Mo(1)–O(5) and Mo(1)–O(2) bond distances were 1.701(3), 1.710(2), 1.860(2), 1.992(2), 2.249(2), and 2.388(2) Å, respectively; oxygen atom sets around Mo2 were one terminal oxygen atom, three double bridging oxygen atoms, one triple bridging oxygen atom, one quadruple bridging oxygen atom; oxygen atom sets around Mo3 were two terminal oxygen atoms, two double bridging oxygen atoms, two triple bridging oxygen atom; oxygen atom sets around Mo4 were one terminal oxygen atom, one double bridging oxygen atom, two triple bridging oxygen atoms, two quadruple bridging oxygen atoms.

Two antisymmetric $[\text{Mo}_4\text{O}_{13}]^{2-}$ units were linked to form a dimeric cage structure $[\text{Mo}_8\text{O}_{26}]^{4-}$ cluster by O12, and then each of the $[\text{Mo}_8\text{O}_{26}]^{4-}$ cluster units extended to construct a scarce one-dimensional catenarian anion structure *via* two bridging O9 atoms linking to each other.^{29a,b} The polyanion catenarian structure exhibited a parallel array along the crystallographic c axis, and organic 1,4-bis(pyridinium)butane cations were orderly arrayed between layers of the one-dimensional chain. Meanwhile, organic cations and polyanions formed an organic–inorganic polyacid supramolecular compound by electrostatic interaction and weak hydrogen bond interaction (Fig. 2b).

In the crystal of compound **4**, the alkyl chain of the 1,6-bis(pyridinium)hexane dication existed in an *anti-anti-gauche-gauche-anti* conformation. The crystal structure of compound **4** was similar to that of compound **2**, and was composed of an independent 1,6-bis(pyridinium)hexane cation and an infinite polyanion $[\text{Mo}_8\text{O}_{26}]^{4-}$ (Fig. S1a–b†). These results suggested that organic cations of $n = 4$ and $n = 6$ have a similar templating effect on the molybdenum oxide anion although they have different alkyl chain lengths.

It is interesting to show another two examples of $[\text{Mo}_8\text{O}_{26}]^{4-}$ isomers induced by di-cationic charged alkyl chain lengths of $n = 4$ $\{[1,1'-(\text{butane-1,4-diyl})\text{bis}(\text{imidazolium})]_2[\delta\text{-Mo}_8\text{O}_{26}]\}^{29c}$ and

$n = 6$ $\{[\text{Me}_3\text{N}(\text{CH}_2)_6\text{NMe}_3][\gamma\text{-Mo}_8\text{O}_{26}]\cdot 2\text{H}_2\text{O}\}$,^{29d} in which the head groups of the di-cations are different, and the $[\text{Mo}_8\text{O}_{26}]$ isomers are also different. So both the head groups and the hydrophobic spacer are important for the template effects.

Structures of [1,5-bis(pyridinium)pentane]₂[θ -Mo₈O₂₆] (3) and [1,8-bis(pyridinium)octane]₂[θ -Mo₈O₂₆] (6) with θ -octamolybdate isomer. In the crystal of compound 3, the alkyl chain of the 1,5-bis(pyridinium)pentane dication existed in an *anti-gauche*₂-*anti* conformation. Single crystal X-ray diffraction analysis revealed that compound 3 was made of an organic 1,5-bis(pyridinium)pentane cation and a polyacid anion θ -[Mo₈O₂₆]⁴⁻ lying about an inversion centre,³⁰ as is shown in Fig. 3a. The cluster may be described as a ring of four [MoO₆] octahedra and two [MoO₅] square pyramids in an edge- and corner-sharing arrangement, capped on either face by tetrahedral {MoO₄} subunits in a corner-sharing mode. The overall structure included 14 terminal-, 8 doubly bridging- and 4 triply bridging-oxo-groups. Then the coordination environment of the Mo atoms and oxygen atoms in 3 was same as that in [Fe(tpyprz)₂]₂[Mo₈O₂₆] \cdot 3.7H₂O,³⁰

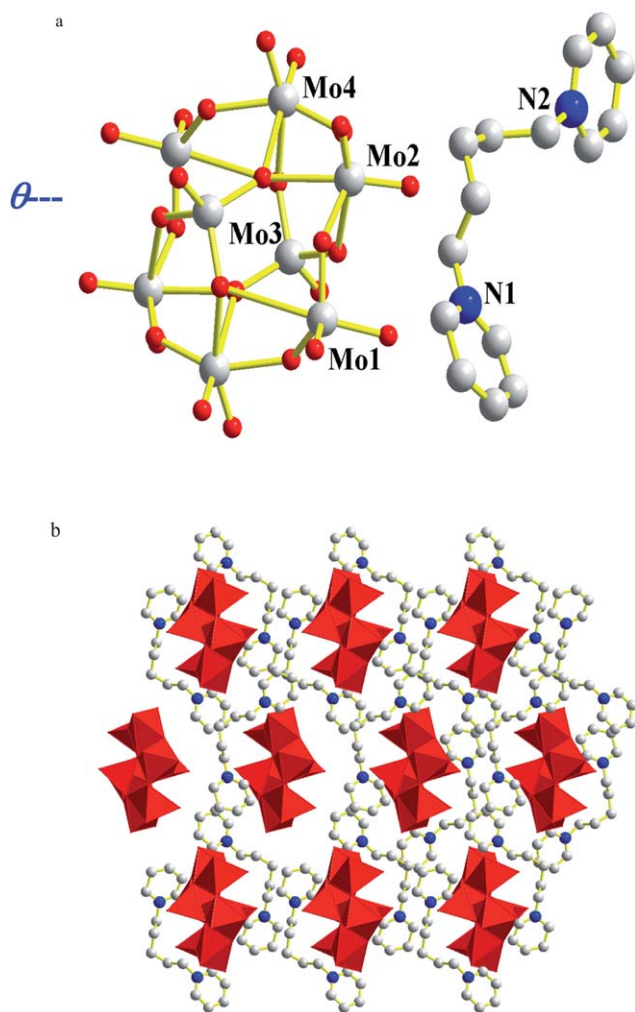


Fig. 3 a Structure of compound 3 with ball and stick style. Symmetry codes: #1 – $x, -y, -z$. All H atoms were omitted for clarity. b Packing structure of compound 3 along the crystallographic c axis. All H atoms were omitted for clarity.

but the bond distances were slightly different. The opposite Mo–Mo distances in the compound 3 were 7.213, 6.692, 6.681, and 3.679 Å, respectively, while the Mo–Mo distances in the [Fe(tpyprz)₂]₂[Mo₈O₂₆] \cdot 3.7H₂O were 7.256, 6.646, 6.509, and 3.669 Å, respectively. The results indicated that the cage structure of compound 3 was bigger and more rounded than [Fe(tpyprz)₂]₂[Mo₈O₂₆] \cdot 3.7H₂O. This θ -polyacid compound with four-coordinated environmental Mo atom is rare.

The packing structure diagram of compound 3 is shown in Fig. 3b. Along the b direction the polyacid [Mo₈O₂₆]⁴⁻ anions together with the organic 1,5-bis(pyridinium)pentane cations exhibit an *ABAB* repeated mode. Along the crystallographic b axis, the polyanions [Mo₈O₂₆]⁴⁻ cluster and the organic cations show a parallel array, and mutually fill each other's interspaces, giving rise to a three-dimensional supramolecular network by electrostatic interactions and intermolecular interactions.

In the crystal of compound 6, the alkyl chain of the 1,8-bis(pyridinium)octane dication existed in an *anti-gauche*-(*anti*)₂-*gauche-anti-anti* conformation. The single crystal X-ray diffraction analysis revealed that compound 6 was made of an organic 1,8-bis(pyridinium)octane cation and a polyacid anion θ -[Mo₈O₂₆]⁴⁻ lying about an inversion centre, as was shown in Fig. S2a–b.† The overall anion cluster structure was similar to that of 3, which indicated that organic 1,5-bis(pyridinium)pentane and 1,8-bis(pyridinium)octane cations have similar templating effects on the assembly of the molybdenum oxide anion. The packing structure diagram of compound 6 is shown in Fig. S2b.† Polyacid [Mo₈O₂₆]⁴⁻ anions exhibited a parallel array in space, and the coupled organic cations showed a tortuous “back to back” shape. Along the crystallographic c axis, organic 1,8-bis(pyridinium)octane cations formed a parallel “Z-shape” chain. Furthermore, polyacid [Mo₈O₂₆]⁴⁻ anions orderly arranged between these “Z-shape” chains, giving rise to an organic–inorganic polyacid supramolecular compound. It is interesting to compare the packing structure of 6 with that of its closely related compound [Fe(tpyprz)₂]₂[Mo₈O₂₆] \cdot 3.7H₂O.³⁰ In the packing structure of the latter, the [Fe(tpyprz)₂]²⁺ complex cation also showed a “Z-shape” chain along the b -axis. This similarity provides further evidence that the [Fe(tpyprz)₂]²⁺ cation possessed an analogous template effect to that of 1,8-bis(pyridinium)octane.

Structures of [1,7-bis(pyridinium)heptane]₂[β -Mo₈O₂₆] (5), [1,10-bis(pyridinium)decane]₂[β -Mo₈O₂₆] (8), and [1,11-bis(pyridinium)undecane]₂[β -Mo₈O₂₆] (9). In the crystal of compound 5, the alkyl chain of the 1,7-bis(pyridinium)heptane dication existed in an *anti*-(*anti*)₃-*gauche-gauche* conformation. Single crystal X-ray diffraction analysis revealed that compound 5 was composed of an independent 1,7-bis(pyridinium)heptane cation and a typical centrosymmetric β -octamolybdate anion [Mo₈O₂₆]⁴⁻³¹ held together by electrostatic interactions (Fig. 4a). The [Mo₈O₂₆]⁴⁻ anion lies about an inversion centre. The β -octamolybdate anion [Mo₈O₂₆]⁴⁻ included two centrosymmetric [Mo₄O₁₃]²⁻ interleaving units linked *via* a bridging oxygen atom. Each [Mo₄O₁₃]²⁻ unit was made up of four MoO₆ edge-sharing octahedra. The oxygen atoms within the [Mo₈O₂₆]⁴⁻ cluster could be divided into four groups according to their bonding features, namely, terminal oxygen atoms with Mo–O distances of 1.691–1.703 Å, double bridging oxygen atoms with Mo–O

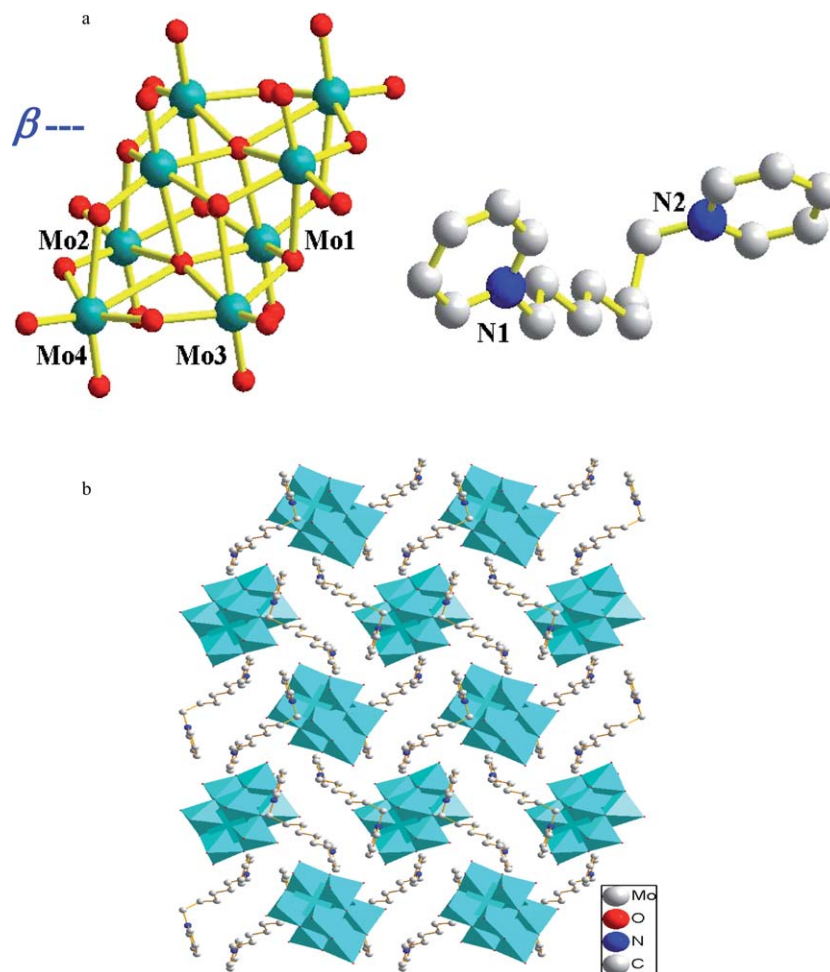


Fig. 4 **a** Structure of compound **5** with ball and stick style. Symmetry codes: #1 $-x + 2, -y, -z + 1$. All H atoms were omitted for clarity. **b** Packing structure of compound **5** with polyhedra ball and stick style along the crystallographic a axis. All H atoms were omitted for clarity.

distances of 1.739(7)–2.277 Å, triple bridging oxygen atoms with Mo–O distances of 1.942(6)–2.356 Å, quintuple bridging oxygen atoms with Mo–O distances of 2.146(6)–2.487(6) Å. The Mo–O average distance of these four groups was 1.697, 1.940, 2.095, and 2.327 Å, respectively. The result showed that these molybdenum oxide polyhedrons were irregular octahedra.

The polyhedral ball and stick packing diagram of **5** viewed down the a axis is shown in Fig. 4b. The polyacid anions $[\text{Mo}_8\text{O}_{26}]^{4-}$ showed a parallel packing arrangement, and the organic cations which acted as the charge balancing component and space-filling component filled in the cavities of the anions cluster, giving rise to an organic–inorganic polyacid supramolecular compound held together by electrostatic interactions and weak hydrogen bond interactions.

In the crystal of compound **8**, the alkyl chain of 1,10-bis(pyridinium)decane dication existed in an *anti-(anti)*₇-*anti* conformation (Fig. S3a–b†), and in the crystal of compound **9**, the alkyl chain of the 1,11-bis(pyridinium)undecane dication existed in an *anti-(anti)*₇-*gauche-anti* conformation (Fig. S4a–b†). Comparably, in compounds **5**, **8** and **9** the $[\text{Mo}_8\text{O}_{26}]^{4-}$ anion lies about an inversion centre, and the distances of the Mo–O bond were only slightly different. These results also indicated that organic cations of $n = 7, 10, 11$ have a similar template effect to the molybdenum oxide anion.

Structure of [1,9-bis(pyridinium)nonane]₂[($\alpha + \beta$)- Mo_8O_{26}] (**7**).

Single crystal X-ray diffraction analysis revealed that compound **7** was composed of two organic 1,9-bis(pyridinium)nonane cations and two independent $[\text{Mo}_8\text{O}_{26}]^{4-}$ anions lying about inversion centres (Fig. 5a). In the crystal of compound **7**, the alkyl chains of two separate 1,9-bis(pyridinium)nonane dications existed in an *anti-(anti)*₃-*gauche-(anti)*₂-*anti* and *anti-(anti)*₂-*gauche-(anti)*₃-*gauche* conformations, respectively. The unit cell consisted of two separate organic cations perpendicularly crossed between two anions. However, the structures of the two polyacid $[\text{Mo}_8\text{O}_{26}]^{4-}$ anions were different. One $[\text{Mo}_8\text{O}_{26}]^{4-}$ anion had a typical α -octamolybdate configuration which was similar to that of compound **1**, the other $[\text{Mo}_8\text{O}_{26}]^{4-}$ anion had a typical β -octamolybdate configuration which was similar to that of compound **5**. The interesting structure contained anions of both α - and β - $[\text{Mo}_8\text{O}_{26}]^{4-}$ configuration, indicating that the compound was evidently a middle transition type, with the alkane modification and the template effect of the organic cation 1,9-bis(pyridinium)nonane integrating the effects of 1,3-bis(pyridinium)propane in **1** and 1,7-bis(pyridinium)heptane in **5**. It was shown that the polyacid anion $[\text{Mo}_8\text{O}_{26}]^{4-}$ took on various structural frameworks for the rational modification of the organic components, and compound **7** featured the first mixed

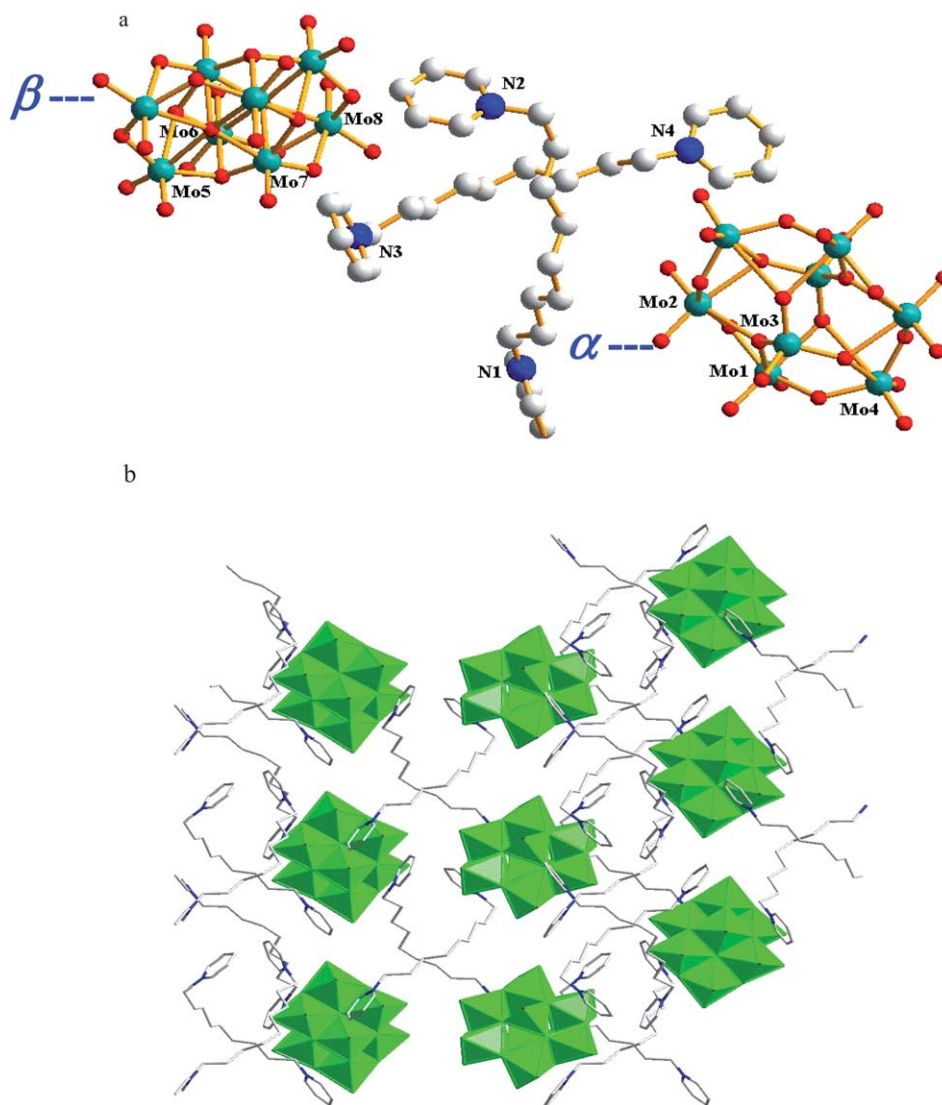


Fig. 5 a Structure of compound **7** as wireframe style. Symmetry codes: #1 $-x + 1, -y, -z + 1$ #2 $-x, -y + 2, -z$. All H atoms were omitted for clarity. b Packing structure of compound **7** along the crystallographic c axis. All H atoms were omitted for clarity.

type $[\text{Mo}_8\text{O}_{26}]^{4-}$ polyoxometalate, so the cation-templating effect played an important role in the preparation of novel organic-inorganic polyacid supramolecular compounds.

Along the crystallographic c axis, the structure of the $[\text{Mo}_8\text{O}_{26}]^{4-}$ anion in every layer was homogeneous while the structure of the $[\text{Mo}_8\text{O}_{26}]^{4-}$ anion in adjacent layers was different, then the α - and β -octamolybdate $[\text{Mo}_8\text{O}_{26}]^{4-}$ anion configuration exhibited an alternative array. The crystal packing of the compound suggested that alternating crossed organic cations filled between parallel layers of anions and formed parallel layered structures. The packing structure diagram of the compound is shown in Fig. 5b.

Structure of [1,12-bis(pyridinium)dodecane] $_2$ $[\gamma\text{-Mo}_8\text{O}_{26}]$ (**10**).

In the crystal of compound **10**, the alkyl chain of the 1,12-bis(pyridinium)dodecane dication existed in an *anti-anti-gauche* (*anti*) $_7$ -*gauche* conformation. Single crystal X-ray diffraction analysis revealed that compound **10** was composed of a organic 1,12-bis(pyridinium)dodecane cation and a rare polyacid

$\gamma\text{-}[\text{Mo}_8\text{O}_{26}]^{4-}$ anion (Fig. 6a).³² The two independent $[\text{Mo}_8\text{O}_{26}]^{4-}$ anions lie about inversion centres. The polyacid anion $[\text{Mo}_8\text{O}_{26}]^{4-}$ possessed a cage structure consisted of an edge-sharing arrangement of six $[\text{MoO}_6]$ octahedra and two $[\text{MoO}_5]$ square pyramids. The oxygen atoms within the $[\text{Mo}_8\text{O}_{26}]^{4-}$ cluster could be divided into four groups according to their bonding features, namely, terminal oxygen atoms with Mo–O distances of 1.639–1.698 Å, double bridging oxygen atoms with Mo–O distances of 1.734–2.377 Å, triple bridging oxygen atoms with Mo–O distances of 1.865–2.453 Å, quadruple bridging oxygen atoms with Mo–O distances of 1.918–2.441 Å. The Mo–O average distance of the four groups was 1.669, 2.056, 2.159, and 2.180 Å, respectively, and the result shows that the MoO_6 octahedra appear slightly distorted.

Along the crystallographic c axis, each polyacid $[\text{Mo}_8\text{O}_{26}]^{4-}$ anion exhibited an alternate layered array, and the crooked organic cation chains with a pyridyl group at either end are connected end-to-end to each other to form an s-shaped chain. Then these organic cations chains extended to form a layered

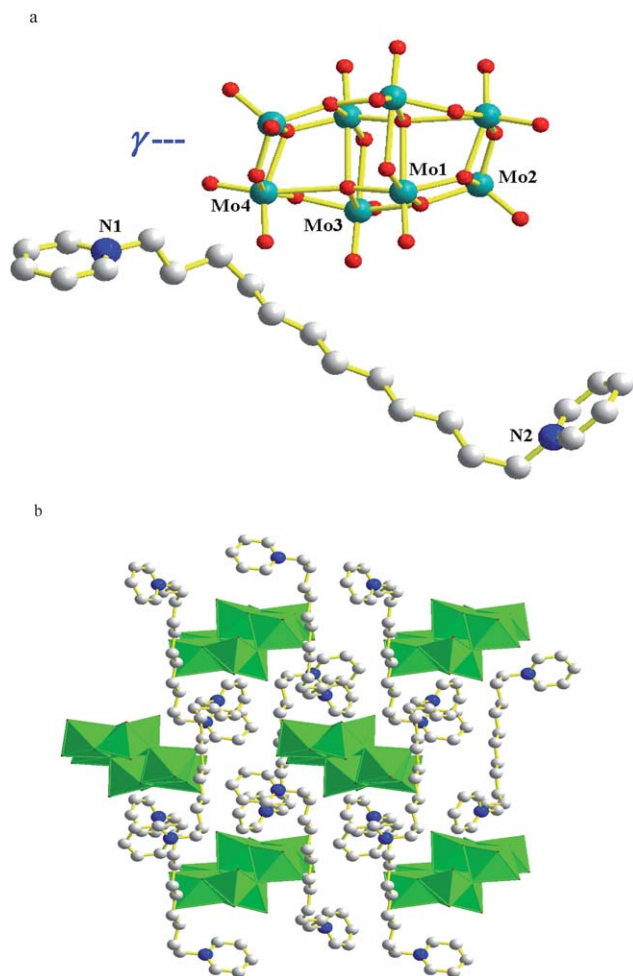


Fig. 6 **a** Structure of compound **10** with ball and stick style. Symmetry codes: #1 $-x, -y + 1, -z$. All H atoms were omitted for clarity. **b** Packing structure of compound **10** along the crystallographic c axis. All H atoms were omitted for clarity.

structure viewed down the a axis, and the polyacid $[\text{Mo}_8\text{O}_{26}]^{4-}$ anions are orderly arrayed between these organic layers. Meanwhile, organic cations and polyacid anions extended to form a three dimensional organic-inorganic supramolecular compound *via* electrostatic interactions and weak intermolecular hydrogen bonds. The packing structure is shown in Fig. 6b. The reported γ - $[\text{Mo}_8\text{O}_{26}]^{4-}$ mainly came from transition metal complex templates,^{32a-d} compound **10** indicated that the bolaamphiphile cation had an integrated effect from the metal and ligands and behaved as a type of excellent supramolecular template.

It is also interesting to compare the influences of the lengths of the alkane from the organic cations on the ultimate packing fashions of these 10 hybrid solids. The cell volumes increase roughly with the growing of the length of the alkyl chain showing the cation size effect. However, compounds **2** and **4** have smaller volumes and compound **7** has a larger one, which are consistent with the anion numbers in the unit cell, and showed that the packing fashion of the anions is inevitably under the influence of that of the cations. This reciprocal template effect from the (+)/(-) moieties also presages a high anion polymeric

dimensionality with the shortening of the lengths of the alkane such as $\omega = 2 \rightarrow 1$ although the two octamolybdate products were not obtained.

IR spectra

In this paper, we used $1,\omega$ -bis(pyridinium) alkane cations as stepwise modification templates and all the anions were $[\text{Mo}_8\text{O}_{26}]^{4-}$; so the IR spectra of the ten compounds were basically similar. The absorption band at about 3400cm^{-1} and 3050cm^{-1} could be assigned to the stretching vibration absorption peak of C-H of the unsaturated carbon atoms. The vibration absorption bands of the aromatic ring appeared in the range of 1650 – 1400cm^{-1} . The band at about 2000cm^{-1} and 1150cm^{-1} corresponded to the stretching vibrations peak of $-\text{CH}_2-$ and C-N. The characteristic absorption bands of the polyacid anion $[\text{Mo}_8\text{O}_{26}]^{4-}$ appeared in the range 1000 – 800cm^{-1} . The sharp absorption bands at 1000 – 800cm^{-1} could be assigned to the stretching vibration of Mo-O, while in the range 800 – 550cm^{-1} could be attributed to the stretching vibration absorption peak of bridging bonds Mo-O_b-Mo. Slight shifts of some peaks come from the template effect of different organic cations and distinguishable polyacid anion configurations.

TGA

In order to investigate the thermal decomposition behavior of **1**–**10**, TGA experiments were carried out up to $800\text{ }^\circ\text{C}$ in a flowing air atmosphere. As is shown in Fig. S5–S14,[†] almost all 10 compounds were thermally stable up to $300\text{ }^\circ\text{C}$. The decomposition of **1**–**6** mainly proceeded in two stages. The first stage took place at the range of $305.0\text{ }^\circ\text{C}$ – $353\text{ }^\circ\text{C}$, which probably corresponded to the elimination of $1,\omega$ -bis(pyridinium)alkane dications; the second stage began at the range of 700 – $740\text{ }^\circ\text{C}$ mainly involved the decomposition of the octamolybdate isomers. The TGA curve for compounds **7**–**10** displays three steps of weight loss. The first and second weight loss began at 290 – $440\text{ }^\circ\text{C}$, corresponding to the decomposition of the long organic cations. The third stage at about $740\text{ }^\circ\text{C}$ mainly involved the collapse of the octamolybdate isomers. Overall, the decomposition temperature of the dications decreased with the growth of the alkane chain length, while all the octamolybdates disintegrated steadily at high temperatures.

Catalytic activities of the compounds

Polyoxometalates (POMs) are known to catalyze the probe reaction for the oxidation of acetaldehyde with H_2O_2 .³³ The catalytic properties of $[\text{Mo}_8\text{O}_{26}]^{4-}$ have been also studied.³⁴ Thus, we decided to test the ability of our POMs to act as oxidation catalysts, and to show preliminary evidence for the effect of variation of the alkane spacer groups on the catalytic properties. The catalytic results diagram is shown in Fig. 7. Under the conditions of the catalysis reactions of these compounds, it was shown that conversion of acetaldehyde was comparatively steady after reacting for 2.5 h. After 3h, the conversions of acetaldehyde were 12.14%, 8.6%, 7.8%, 10.2%, 8.0%, 7.13%, 6.86%, 6.5%, 6.3%, respectively. Under the same experimental conditions, the title compounds showed an acetic acid formation rate of 40.47, 28.67, 26.00, 26.93, 34.03, 23.77, 22.90, 21.67, 21.00 mmol

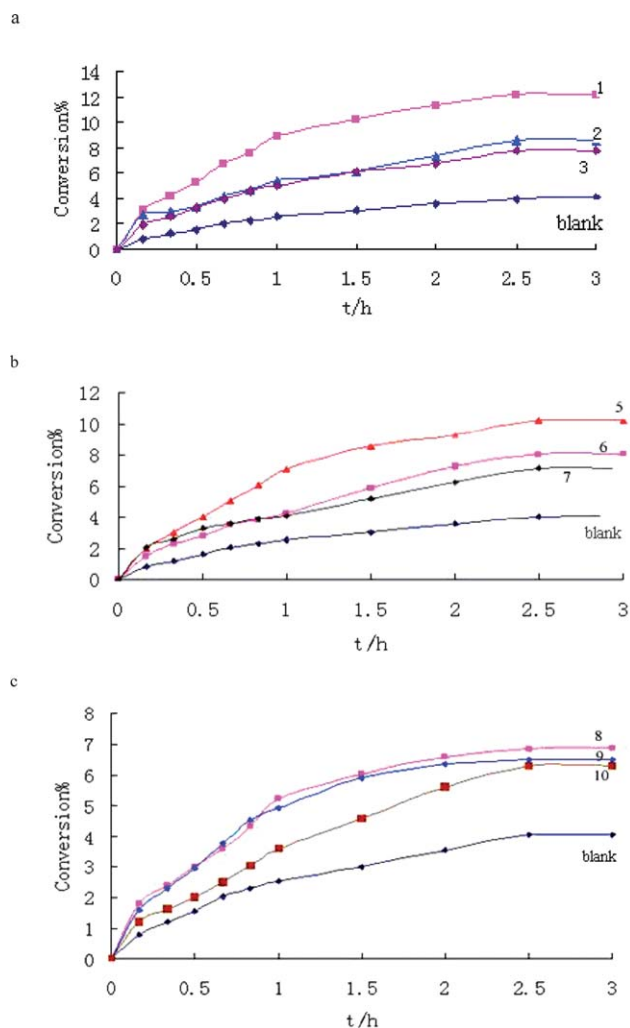


Fig. 7 Conversion versus time plot of catalytic oxidation of acetaldehyde with H_2O_2 . (a) Catalytic results with **1**, **2**, and **3** as catalyst. (b) Catalytic results with **5**, **6**, and **7** as catalyst. (c) Catalytic results with **8**, **9**, and **10** as catalyst.

(g-cat.) $^{-1}$ h $^{-1}$, respectively, while $\text{Ni}_2\text{Al-CO}_3$, *i. e.* the clay catalyst $\text{Ni}_{0.7}\text{Al}_{0.3}(\text{OH})_2 \cdot 0.15\text{CO}_3 \cdot 0.86\text{H}_2\text{O}$, has an activity of 8.0 mmol (g-cat.) $^{-1}$ h $^{-1}$.^{33a} The catalytic activity shows an increase of around 2.62–5.05 times for the title compounds over $\text{Ni}_2\text{Al-CO}_3$. These POMs may thus be good candidates for oxidative catalysts in some other organic reactions.

However, the most active catalysts seem to be those that contained short alkane spacers. The catalytic activities decrease with the increase of the length of the alkyl chain in the 1, ω -bis-(pyridinium) alkanes. We deduced that long organic cations were probably adverse to the electron transmission in the oxidation–reduction reaction. These results clearly show differences in catalytic activity which can be attributed to alkane spacer groups with varying electron transfer abilities. One possible scenario is that the short alkane chain and cation size bring large flexibility and electron transfer abilities in solution, which facilitates the interaction with the peroxide *via* hydrogen bonding³⁵ (among CH_2 , $[\text{Mo}_8\text{O}_{26}]^{4-}$ and H_2O_2), the activation of H_2O_2 and the cleavage of the peroxide O–O bond. In short, the catalytic activities of these POMs seem to be modulated by the

alkane groups of the cation. Thus, detailed studies on the mechanism of peroxide activation of these POMs are warranted and are being conducted in our laboratory.

Experimental section

Materials and methods

The dications $[\text{Py}-(\text{CH}_2)_n-\text{Py}]^{2+}$ ($n = 3-12$) were prepared as the bromide salts by direct alkylation of pyridine with 1, ω -dibromoalkane. Other chemicals were obtained from commercial sources and used as received without further purification. The IR spectrum was recorded on a Shimadzu IR435 spectrometer as KBr disk (4000–400 cm^{-1}). Elemental analyses (C, H, and N) were carried out on a FLASH EA 1112 elemental analyzer. The purity of the bulk microcrystalline materials obtained from the syntheses was checked by Powder X-ray diffraction analyses. XRPD patterns were recorded using Cu-K α 1 radiation on a PAN analytical X'Pert PRO diffractometer. A model NETZSCHTG209 thermal analyzer was used to record simultaneous TG, DTG curves in a flowing air atmosphere of 20 mL min^{-1} at a heating rate of 5 $^\circ\text{C min}^{-1}$ in the temperature range 0–850 $^\circ\text{C}$ using platinum crucibles.

Compound syntheses

[1,3-Bis(pyridinium)propane] $_2$ [α - Mo_8O_{26}] (1**).** A mixture of $(\text{NH}_4)_6\text{Mo}_7\text{O}_{24} \cdot 4\text{H}_2\text{O}$ (0.0617 g, 0.05 mmol), [1,3-bis(pyridinium)propane] $\cdot 2\text{Br}$ (0.0540 g, 0.15 mmol), and H_2O (10 mL) was stirred for 20 min in air until it was homogeneous. The mixture was sealed in a 23 mL Teflon-lined stainless steel container, which was heated to 120 $^\circ\text{C}$ under autogenous pressure for 3 d. After the mixture was cooled to room temperature at 10 $^\circ\text{C h}^{-1}$, light yellow green crystals of **1** were obtained, Yield: 54%. Anal. calcd (%) for $\text{C}_{26}\text{H}_{32}\text{Mo}_8\text{N}_4\text{O}_{26}$: C 19.72, H 2.01, N 3.54 found: C 19.61, H 2.36, N 3.55; IR (KBr, cm^{-1}): 3444 (s), 3062 (m), 1632 (s), 1490 (m), 913 (s), 804 (s), 670 (s), 569 (m).

[1,4-Bis(pyridinium)butane] $_2$ [$\text{D-Mo}_8\text{O}_{26}$] (2**).** Compound **2** was synthesized similarly to compound **1** by using [1,4-bis(pyridinium)butane] $\cdot 2\text{Br}$ (0.0561 g, 0.15 mmol) instead of [1,3-bis(pyridinium)propane] $\cdot 2\text{Br}$. Then the mixture was heated to 120 $^\circ\text{C}$ under autogenous pressure for 4 d. Light green rod crystals of **2** were obtained in a 52% yield. Anal. calcd (%) for $\text{C}_{14}\text{H}_{18}\text{Mo}_4\text{N}_2\text{O}_{13}$: C 20.87, H 2.26, N 3.48 found: C 20.71, H 2.36, N 3.58; IR (KBr, cm^{-1}): 3745 (s), 1630 (s), 1483 (m), 1273 (m), 1173 (m), 937 (m), 864 (m), 622 (s), 480 (s).

[1,5-Bis(pyridinium)pentane] $_2$ [θ - Mo_8O_{26}] (3**).** Compound **3** was synthesized similarly to compound **1** by using [1,5-bis(pyridinium)pentane] $\cdot 2\text{Br}$ (0.0582 g, 0.15 mmol) instead of [1,3-bis(pyridinium)propane] $\cdot 2\text{Br}$. Then the mixture was heated to 150 $^\circ\text{C}$ under autogenous pressure for 4d. The resulting colorless crystals of **3** were formed, yield: 58%. Anal. calcd (%) for $\text{C}_{15}\text{H}_{20}\text{Mo}_4\text{N}_2\text{O}_{13}$: C 21.98, H 2.45, N 3.42 found: C 21.81, H 2.66, N 3.74; IR (KBr, cm^{-1}): 3447(s), 1632 (s), 1490 (m), 921 (s), 800 (s), 658 (s), 552 (m).

[1,6-Bis(pyridinium)hexane] $_2$ [$\text{D-Mo}_8\text{O}_{26}$] (4**).** A mixture of $(\text{NH}_4)_6\text{Mo}_7\text{O}_{24} \cdot 4\text{H}_2\text{O}$ (0.0617 g, 0.05 mmol),

[1,6-bis(pyridinium)hexane]·2Br (0.0603 g, 0.15 mmol), and H₂O (10 mL) was adjusted with dilute HNO₃ to pH 3–3.5. Then, the mixture was placed in a 23 mL Teflon-lined autoclave and kept under autogenous pressure at 160 °C for 4 days. After it was gradually cooled to room temperature at a rate of 10 °C h⁻¹, colorless crystals of **4** were obtained. Yield: 48%. Anal. calcd (%) for C₁₆H₂₂Mo₄N₂O₁₃: C 23.03, H 2.65, N 3.36 found: C 23.61, H 2.76, N 3.43; IR (KBr, cm⁻¹): 3454(s), 3057(s), 2928(m), 1629(s), 1484(s), 1165(s), 926(s), 865(s), 761(s), 482(s).

[1,7-Bis(pyridinium)heptane]₂[β-Mo₈O₂₆] (5). Compound **5** was synthesized similarly to compound **4** by using [1,7-bis(pyridinium)heptane]·2Br (0.0416 g, 0.1 mmol) instead of [1,6-bis(pyridinium)hexane]·2Br. Colorless crystals of **5** were formed, yield: 50%. Anal. calcd (%) for C₃₄H₄₈Mo₈N₄O₂₆: C 24.08, H

2.83, N 3.30 found: C 24.31, H 2.76, N 3.32; IR (KBr, cm⁻¹): 3448 (s), 3060 (s), 1626 (s), 1484 (s), 1188 (m), 941 (s), 848 (s), 716 (s), 552 (m).

[1,8-Bis(pyridinium)octane]₂[θ-Mo₈O₂₆] (6). Compound **6** was synthesized similarly to compound **4** by using [1,8-bis(pyridinium)octane]·2Br (0.0430 g, 0.1 mmol) instead of [1,6-bis(pyridinium)hexane]·2Br. Colorless crystals of **6** were formed, yield: 60%. Anal. calcd (%) for C₃₆H₅₂Mo₈N₄O₂₆: C 25.08, H 3.04, N 3.25 found: C 25.61, H 3.16, N 3.41; IR (KBr, cm⁻¹): 3448 (s), 3062 (s), 2973 (m), 1629 (s), 1485 (s), 1314 (s), 1173 (s), 911 (s), 804 (s), 659 (s), 550 (m).

[1,9-Bis(pyridinium)nonane]₂[(α + β)-Mo₈O₂₆] (7). Compound **7** was synthesized similarly to compound **4** by using

Table 1 Crystal data and structure refinement details for 1–10

	1	2	3	4	5
Formula	C ₂₆ H ₃₂ Mo ₈ N ₄ O ₂₆	C ₁₄ H ₁₈ Mo ₄ N ₂ O ₁₃	C ₁₅ H ₂₀ Mo ₄ N ₂ O ₁₃	C ₁₆ H ₂₂ Mo ₄ N ₂ O ₁₃	C ₃₄ H ₄₈ Mo ₈ N ₄ O ₂₆
Formula weight	1584.08	806.06	820.09	834.12	1696.28
Cryst. syst.	Monoclinic	Triclinic	Monoclinic	Triclinic	Monoclinic
Space group	<i>P</i> 2 ₁ / <i>n</i>	<i>P</i> -1	<i>P</i> 2 ₁ / <i>n</i>	<i>P</i> -1	<i>P</i> 2 ₁ / <i>n</i>
<i>a</i> /Å	10.2659(4)	9.6800(6)	10.434(2)	9.6722(6)	11.2831(7)
<i>b</i> /Å	20.0891(8)	10.4525(6)	20.632(4)	9.8924(6)	18.3289(11)
<i>c</i> /Å	10.3756(4)	12.2127(8)	11.583(2)	12.7236(8)	11.9515(7)
α/°	90	65.7660(10)	90	105.8290(10)	90
β/°	100.6330(10)	79.8680(10)	107.98(3)	94.8730(10)	90.8730(10)
γ/°	90	70.7540(10)	90	95.7600(10)	90
Vol/Å ³	2102.99(14)	1062.63(11)	2371.8(8)	1157.28(12)	2471.4(3)
<i>Z</i>	2	2	4	2	2
<i>D</i> _c /g cm ⁻³	2.502	2.519	2.297	2.394	2.280
μ/mm ⁻¹	2.401	2.378	2.133	2.188	2.051
<i>F</i> (000)	1520	776	1584	808	1648
Rflns collected	13326	5654	7445	6766	13501
Unique rflns	4802	3685	3914	4463	4594
<i>R</i> _{int}	0.0211	0.0143	0.0330	0.0122	0.0148
GOF	1.041	1.056	1.097	1.037	1.060
<i>R</i> ₁ ^a (<i>I</i> > 2σ(<i>I</i>))	0.0254	0.0222	0.0549	0.0263	0.0216
<i>wR</i> ₂ ^a (all data)	0.0646	0.0656	0.1358	0.0635	0.0600
Δρmax/Δρmin/e Å ⁻³	1.556/−1.630	0.918/−0.650	1.144/−1.931	1.014/−0.623	0.614/−0.945
	6	7	8	9	10
Formula	C ₃₆ H ₅₂ Mo ₈ N ₄ O ₂₆	C ₇₆ H ₁₁₂ Mo ₁₆ N ₈ O ₅₂	C ₄₀ H ₆₀ Mo ₈ N ₄ O ₂₆	C ₄₂ H ₆₄ Mo ₈ N ₄ O ₂₆	C ₄₄ H ₆₈ Mo ₈ N ₄ O ₂₆
Formula weight	1724.34	3504.78	1780.44	1808.49	1836.54
Cryst. syst.	Monoclinic	Monoclinic	Monoclinic	Monoclinic	Monoclinic
Space group	<i>P</i> 2 ₁ / <i>n</i>	<i>P</i> 2 ₁ / <i>n</i>	<i>P</i> 2 ₁ / <i>n</i>	<i>P</i> 2 ₁ / <i>n</i>	<i>P</i> 2 ₁ / <i>n</i>
<i>a</i> /Å	15.5447(8)	22.684(2)	11.1947(8)	12.5763(8)	12.5475(7)
<i>b</i> /Å	10.1543(5)	13.1384(12)	17.5265(13)	13.0193(9)	16.7311(10)
<i>c</i> /Å	16.6922(8)	19.4278(17)	14.1876(10)	17.6460(12)	14.5205(8)
α/°	90	90	90	90	90
β/°	90.0590(10)	108.6190(10)	97.3510(10)	99.0140(10)	97.3650(10)
γ/°	90	90	90	90	90
Vol/Å ³	2634.8(2)	5487.0(8)	2760.8(3)	2853.6(3)	3023.2(3)
<i>Z</i>	2	2	2	2	2
<i>D</i> _c /g cm ⁻³	2.173	2.121	2.142	2.105	2.018
μ/mm ⁻¹	1.926	1.851	1.842	1.783	1.685
<i>F</i> (000)	1680	3424	1744	1776	1808
Rflns collected	14302	29522	15100	15439	16634
Unique rflns	4901	10100	5137	5273	5618
<i>R</i> _{int}	0.0173	0.0246	0.0380	0.0175	0.0173
GOF	1.069	1.053	1.050	1.107	1.034
<i>R</i> ₁ ^a (<i>I</i> > 2σ(<i>I</i>))	0.0254	0.0915	0.0299	0.0211	0.0231
<i>wR</i> ₂ ^a (all data)	0.0641	0.2427	0.0825	0.0542	0.0567
Δρmax/Δρmin/e Å ⁻³	0.971/−0.814	12.800/−2.107	0.591/−0.965	0.327/−0.666	1.183/−0.673

^a *R*₁ = ||*F*_o|| − ||*F*_c||/||*F*_o||; *wR*₂ = [w(*F*_o² − *F*_c²)/w(*F*_o²)]^{1/2}.

[1,9-bis(pyridinium)nonane]·2Br (0.0444 g, 0.1 mmol) instead of [1,6-bis(pyridinium)hexane]·2Br. Colorless crystals of **7** were formed, yield: 54%. Anal. calcd (%) for $C_{76}H_{112}Mo_{16}N_8O_{52}$: C 26.05, H 3.21, N 3.20 found: C 26.21, H 3.56, N 3.30; IR (KBr, cm^{-1}): 3449 (s), 3064 (s), 2926 (s), 1628 (s), 1484 (s), 1170 (m), 912 (s), 805 (s), 663 (s), 552 (m).

[1,10-Bis(pyridinium)decane]₂[β -Mo₈O₂₆] (8). Compound **8** was synthesized similarly to compound **4** by using [1,10-bis(pyridinium)decane]·2Br (0.0458 g, 0.1 mmol) instead of [1,6-bis(pyridinium)hexane]·2Br. Colorless crystals of **8** were formed, yield: 58%. Anal. calcd (%) for $C_{40}H_{60}Mo_8N_4O_{26}$: C 26.98, H 3.40, N 3.15 found: C 26.61, H 3.56, N 3.32; IR (KBr, cm^{-1}): 3430 (s), 3060 (s), 2926 (m), 1628 (s), 1485 (s), 1168 (s), 946 (s), 844 (s), 714 (s), 556 (m).

[1,11-Bis(pyridinium)undecane]₂[β -Mo₈O₂₆] (9). Compound **9** was obtained similarly to compound **4** by using [1,11-bis(pyridinium)undecane]·2Br (0.0470 g, 0.1 mmol) instead of [1,6-bis(pyridinium)hexane]·2Br. Colorless crystals of **9** were formed, yield: 52%. Anal. calcd (%) for $C_{42}H_{64}Mo_8N_4O_{26}$: C 27.88, H 3.56, N 3.10 found: C 27.61, H 3.76, N 3.27; IR (KBr, cm^{-1}): 3444 (s), 3058 (s), 2925 (m), 1630 (s), 1484 (s), 1172 (s), 940 (s), 909 (s), 711 (s), 520 (m).

[1,12-Bis(pyridinium)dodecane]₂[γ -Mo₈O₂₆] (10). Compound **10** was prepared similarly to compound **4** by using [1,12-bis(pyridinium)dodecane]·2Br (0.0486 g, 0.1 mmol) instead of [1,6-bis(pyridinium)hexane]·2Br. Colorless crystals of **10** were formed, yield: 54%. Anal. calcd (%) for $C_{44}H_{68}Mo_8N_4O_{26}$: C 28.76, H 3.74, N 3.05 found: C 28.06, H 3.86, N 3.47; IR (KBr, cm^{-1}): 3444 (s), 3060 (s), 2924 (m), 1710 (m), 1631 (s), 1487 (s), 1172 (m), 907 (s), 794 (s), 659 (s).

X-Ray crystallography

Crystallographic data for the ten compounds was collected on a Bruker APEX-II area-detector diffractometer with Mo-K α radiation ($\lambda = 0.71073$). Absorption corrections were applied by using SADABS. The structures were solved with direct methods and refined with full-matrix least-squares techniques on F^2 using the SHELXTL program package. All of the non-hydrogen atoms were refined anisotropically. The hydrogen atoms were assigned with common isotropic displacement factors and included in the final refinement by using geometrical restraints. In **7** the large residual electron density peak was located close to (1.3 Å from) the Mo atom and was most likely due to imperfect absorption corrections frequently encountered in heavy-metal atom structures. Crystal data for **1–10** were summarized in detail in Table 1. Selected bond lengths and bond angles were put in Table S1.† In order to confirm the phase purity of the bulk materials, X-ray powder diffraction (XRPD) experiments were carried out for compounds **1–10**. The experimental PXRD patterns of **1–10** correspond well to the simulated PXRD patterns, indicating that the bulk phase materials are isomorphous. The difference in reflection intensities between the simulated and experimental patterns was due to the variation in the preferred orientation of the powder sample during collection of the experimental PXRD data (Fig. S15–S24†).

Catalysis oxidation reactions of acetaldehyde to acetic acid

In this article, we selected the oxidation reaction of acetaldehyde to acetic acid as a model reaction in order to measure the catalytic oxidation activities of these compounds. A mixture of acetaldehyde (0.05 mol, 5.7 ml, 40%) and H₂O₂ (0.1 mol, 10 ml, 30%) was placed in a three-neck flask (50 ml) at room temperature, stirred and heated to 60 °C, then the catalyst (0.05 g) that was one of the above compounds was added into the mixture and the reaction was retained in the range 50–60 °C, refluxing for 3 h. The sampling frequency at the beginning of the reaction was once every 10 min, then once every 30 min 1 h later. The final solution was titrated with standard NaOH solution and the conversion ratio of acetaldehyde was calculated. The formation rate of the ethanoic acid produced [$mmol(g\text{-cat})^{-1}h^{-1}$] was taken in order to assess the catalytic activity.

Conclusion

Aiming at crystal engineering with nanosized POM building blocks we succeeded in preparing ten novel inorganic–organic hybrid octamolybdate supramolecular isomers by modification of 1, ω -bis(pyridinium) alkane dications acting as permanent templates.³⁶ The templates filling in cavities of polyacid anions not only play the role of charge compensation and direct the packing motif, more importantly, it also significantly influences the structure of the POM framework, and some unprecedented POMs were expected as components of hybrids with cation templates. In these ten compounds, the octamolybdate anion [Mo₈O₂₆]⁴⁻ of compounds **2** and **4** both had a one-dimensional catenarian structure, while the others were of a different cage structure. Compound **1** contained the discrete α -[Mo₈O₂₆]⁴⁻ clusters, while the octamolybdate anion [Mo₈O₂₆]⁴⁻ was always the typical β -[Mo₈O₂₆]⁴⁻ cluster in compound **5**, **8** and **9**. In compound **3** and **6**, the octamolybdate anion [Mo₈O₂₆]⁴⁻ was an ellipsoid shaped cage structure and belonged to the scarce θ -[Mo₈O₂₆]⁴⁻ cluster. An interesting structure of polyacid [Mo₈O₂₆]⁴⁻ anions in compound **7** contained both the anion structure of compound **1** and compounds **5**, **8**, **9**, showing that the compound **7** was a middle transition type. Compound **10** contained the unusual γ -[Mo₈O₂₆]⁴⁻ clusters and looked like a flat cage structure. Consequently, we demonstrated that these polyacid [Mo₈O₂₆]⁴⁻ anions took on various isomeric frameworks for the fine modification of organic components. Therefore, cation-templated effects played an important role in the preparation of novel organic–inorganic polyacid supramolecular compounds. Moreover, it was indicated that all these polyacid compounds had definite catalytic activities in some organic oxidation reactions and the catalytic activities were related to the length of the alkyl chain in 1, ω -bis(pyridinium) alkanes.

Acknowledgements

Research efforts in the Niu group are supported by the National Science Foundation of China (No. 20671083).

References

- 1 S. I. Stupp and P. V. Braun, *Science*, 1997, **277**, 1242.

- 2 P. V. Braun, P. Osenar, V. Tohver, S. B. Kennedy and S. I. Stupp, *J. Am. Chem. Soc.*, 1999, **121**, 7302–7309.
- 3 A. Müller, S. Q. N. Shah, H. Bögge and M. Schmidtman, *Nature*, 1999, **397**, 48–50.
- 4 M. J. Zaworotko, *Angew. Chem., Int. Ed.*, 1998, **37**, 1211.
- 5 (a) M. C. Hong, *Cryst. Growth Des.*, 2007, **7**(1), 10–14; (b) C. L. Hill, *Chem. Rev.*, 1998, **98**, 1.
- 6 A. K. Cheetham, G. Ferey and T. Loiseau, *Angew. Chem., Int. Ed.*, 1999, **38**, 3268–3292.
- 7 X. L. Wang, C. Qin, E. B. Wang, Y. G. Li, C. W. Hu and L. Xu, *Chem. Commun.*, 2004, 378–379.
- 8 (a) M. Sadakane, M. H. Dickman and M. T. Pope, *Angew. Chem., Int. Ed.*, 2000, **39**, 2914; (b) X. M. Zhang, M. L. Tong and X. M. Chen, *Chem. Commun.*, 2000, 1817–1818.
- 9 (a) C.-M. Liu, Y.-L. Hou, J. Zhang and S. Gao, *Inorg. Chem.*, 2002, **41**, 140–143; (b) C.-D. Wu, C.-Z. Lu, X. Lin, D.-M. Wu, S.-F. Lu, H.-H. Zhuang and J.-S. Huang, *Chem. Commun.*, 2003, 1284–1285; (c) J.-R. Li, X.-H. Bu and R.-H. Zhang, *Inorg. Chem.*, 2004, **43**, 237–244.
- 10 (a) U. Kortz, M. G. Savelieff, F. Y. Abou Ghali, L. M. Khalil, S. A. Maalouf and D. I. Sinno, *Angew. Chem., Int. Ed.*, 2002, **41**, 4070; (b) C. D. Peloux, P. Mialane, A. Dolbecq, J. Marrot and F. Sécheresse, *Angew. Chem., Int. Ed.*, 2002, **41**, 2808–2810; (c) C. Z. Wu, H. H. Lu and J. S. Zhuang, *J. Am. Chem. Soc.*, 2002, **124**, 3836–3837.
- 11 (a) A. Müller and C. Serain, *Acc. Chem. Res.*, 2000, **33**, 2–10; (b) D. L. Long and L. Cronin, *Chem.–Eur. J.*, 2006, **12**, 3698–3706.
- 12 M. Hölscher, U. Englert, B. Zibrowius and W. F. Hölderich, *Angew. Chem., Int. Ed. Engl.*, 1995, **33**, 2491–2493.
- 13 (a) E. Coronado, J. R. Gamenez-Saiz, C. J. Gomez-Garcia, L. R. Falvello and P. Delaes, *Inorg. Chem.*, 1998, **37**, 2183–2188; (b) A. R. Moore, H. Kwen, A. M. Beatty and E. A. Maatta, *Chem. Commun.*, 2000, 1793–1794.
- 14 L. Xu, M. Lu, B. B. Xu, Y. G. Wei, Z. H. Peng and D. Powell, *Angew. Chem., Int. Ed.*, 2002, **41**, 4129–4132.
- 15 Y. G. Li, N. Hao, E. B. Wang, M. Yuan, C. W. Hu, N. H. Hu and H. Q. Jia, *Inorg. Chem.*, 2003, **42**, 2729–2735.
- 16 (a) C. T. Kressge, M. E. Leonowicz, W. J. Roth, J. C. Vartuni and J. S. Beck, *Nature*, 1992, **359**, 710; (b) E. Coronado and C. J. Gomez-Garcia, *Chem. Rev.*, 1998, **98**, 273–296.
- 17 (a) Y. Du, A. L. Rheingold and E. A. Maatta, *J. Am. Chem. Soc.*, 1992, **114**, 346–348; (b) R. Proust, M. Thouvenot, F. Chaussade, F. Robert and P. Gouzerh, *Inorg. Chim. Acta*, 1994, **224**, 81–95.
- 18 D. Hagrman, C. Zubieta, R. C. Haushalter and J. Zubieta, *Angew. Chem., Int. Ed. Engl.*, 1997, **36**, 873.
- 19 D. G. Allis, R. S. Rarig, E. Burkholder and J. Zubieta, *J. Mol. Struct.*, 2004, **688**, 11–31.
- 20 A. J. Bridgeman, *J. Phys. Chem. A*, 2002, **106**, 12151–12160.
- 21 D. G. Allis, E. Burkholder and J. Zubieta, *Polyhedron*, 2004, **23**, 1145–1152.
- 22 C. D. Wu, C. Z. Lu, H. H. Zhuang and J. S. Huang, *Inorg. Chem.*, 2002, **41**, 5636.
- 23 D. Hagrman, P. J. Zapf and J. Zubieta, *Chem. Commun.*, 1998, (12), 1283.
- 24 D. R. Xiao, Y. Hou, E. B. Wang, S. T. Wang, Y. G. Li, L. Xu and C. W. Hu, *Inorg. Chim. Acta*, 2004, **357**, 2525–2531.
- 25 R. S. Rarig and J. Zubieta, *Inorg. Chim. Acta*, 2001, **312**, 188–196.
- 26 J. P. Wang, S. Z. Li, J. W. Zhao and J. Y. Niu, *Inorg. Chem. Commun.*, 2006, **9**, 599–602.
- 27 Y. Y. Niu, B. L. Wu, X. L. Guo, Y. L. Song, X. C. Liu, H. Y. Zhang, H. W. Hou, C. Y. Niu and S. W. Ng, *Cryst. Growth Des.*, 2008, **8**, 2393–2401.
- 28 (a) R. S. Rarig Jr., L. Bewley, V. Golub, C. J. O'Connor and J. Zubieta, *Inorg. Chem. Commun.*, 2003, **6**, 539; (b) P. J. Hagrman and J. Zubieta, *Inorg. Chem.*, 1999, **38**, 4480.
- 29 (a) P. J. Hagrman, D. Hagrman and J. Zubieta, *Angew. Chem., Int. Ed.*, 1999, **38**, 2638–2684; (b) K. J. Thorn, A. Narducci Sarjeant and A. J. Norquist, *Acta Crystallogr., Sect. E: Struct. Rep. Online*, 2005, **61**, m1665–m1667; (c) R. Dessapt, D. Kervern, M. Bujoli-Doeuff, P. Deniard, M. Evain and S. Jobic, *Inorg. Chem.*, 2010, **49**, 11309–11316; (d) H. G. Hou and J. L. Yang, *Acta Crystallogr., Sect. E: Struct. Rep. Online*, 2007, **63**, m2194; (e) M. L. Niven, J. J. Cruywagen, J. Bernard and B. Heynes, *J. Chem. Soc., Dalton Trans.*, 1991, (8), 2007.
- 30 D. G. Allis, E. Burkholder and J. Zubieta, *Polyhedron*, 2004, **23**, 1145.
- 31 (a) S. Upreti and A. Ramanan, *Cryst. Growth Des.*, 2005, **5**(5), 1837–1843; (b) T. Duraisamy, A. Ramanan and J. J. Vittal, *J. Mater. Chem.*, 1999, **9**, 763–767.
- 32 (a) C. D. Wu, C. Z. Lu, S. M. Chen, H. H. Zhuang and J. S. Huang, *Polyhedron*, 2003, **22**, 3091; (b) J. R. D. DeBord, R. C. Haushalter, L. M. Meyer, D. J. Rose, P. J. Zapf and J. Zubieta, *Inorg. Chim. Acta*, 1997, **256**, 165; (c) R. S. Rarig Jr., P. J. Hagrman and J. Zubieta, *Solid State Sci.*, 2002, **4**, 77; (d) X. B. Cui, K. Lii, Y. Fan, J. Q. Xu, L. Ye, Y. H. Sun, Y. Li, H. H. Yu and Z. H. Yi, *J. Mol. Struct.*, 2005, **743**, 151.
- 33 (a) C. W. Hu, X. Zhang, L. Xu, B. L. Mu, W. Zu and E. B. Wang, *Appl. Clay Sci.*, 1998, **13**, 495–511; (b) R. Bagtache, K. Abdmeziem, S. Boutamine, M. Meklati and O. Vittori, *Synth. React. Inorg., Metal-Org., Nano-Metal Chem.*, 2009, **39**, 467–474; (c) L. Xu, Y. Q. Sun, E. B. Wang, E. H. Shen, Z. R. Liu, C. W. Hu, Y. Xing, Y. H. Lin and H. Q. Jia, *Inorg. Chem. Commun.*, 1998, **1**, 382–385; (d) L. Xu, Y. Q. Sun, E. B. Wang, E. H. Shen, Z. R. Liu, C. W. Hu, Y. Xing, Y. H. Lin and H. Q. Jia, *New J. Chem.*, 1999, **23**, 1041–1044; (e) B. Z. Lin, G. H. Han, B. H. Xu, L. Bai, Y. L. Feng and H. Su, *J. Cluster Sci.*, 2008, **19**, 379–390; (f) L. Xu, Y. Q. Sun, E. B. Wang, E. H. Shen, Z. R. Liu and C. W. Hu, *Transition Met. Chem.*, 1999, **24**, 492–495; (g) L. Xu, Y. Q. Sun, E. B. Wang, E. H. Shen, Z. R. Liu and C. W. Hu, *J. Solid State Chem.*, 1999, **146**, 533–537.
- 34 (a) M. L. Guo and H. Z. Li, *Green Chem.*, 2007, **9**, 421–423; (b) C. B. Yang, Q. P. Jin, H. Zhang, J. Liao, J. Zhu, B. Yu and J. G. Deng, *Green Chem.*, 2009, **11**, 1401–1405.
- 35 (a) C. J. Chang, L. L. Chng and D. G. Nocera, *J. Am. Chem. Soc.*, 2003, **125**, 1866–1876; (b) J. D. Soper, S. V. Kryatov, E. V. Rybak-Akimova and D. G. Nocera, *J. Am. Chem. Soc.*, 2007, **129**, 5069–5075; (c) V. G. Organo, A. S. Filatov, J. S. Quartararo, Z. M. Friedman and E. V. Rybak-Akimova, *Inorg. Chem.*, 2009, **48**, 8456–8468.
- 36 H. Ralf and V. Fritz, *Angew. Chem., Int. Ed. Engl.*, 1994, **33**, 375.